Journal of Solid Mechanics Vol. 12, No. 1 (2020) pp. 57-71
DOI: 10.22034/jsm.2019.582849.1371

Hygrothermal Creep and Stress Redistribution Analysis of Temperature and Moisture Dependent Magneto-Electro-Elastic Hollow Sphere

M. Saadatfar*

Department of Mechanical Engineering, University of Qom, Qom, Iran

Received 3 September 2019; accepted 8 December 2019

ABSTRACT

In this article, the time-dependent stress redistribution analysis of magneto-electro-elastic (MEE) thick-walled sphere subjected to mechanical, electrical, magnetic and uniform temperature gradient as well as moisture concentration gradient is presented. Combining constitutive equations of MEE with stress-strain relations as well as strain-displacement relations results in obtaining a differential equation in which there are the creep strains. At the first step, discounting creep strains in the mentioned equation, an analytical solution for the hygro-thermo-magneto-electro-elastic behavior is achieved at the initial state. After that, the creep stress rates can be achieved by keeping only the creep strains in the differential equation for the steady-state condition. The analysis is done by applying the Prandtl-Reuss equations as well as Norton's law in creep behavior modeling. Finally, the history of stresses, displacement as well as magnetic and potential field, at any time, is achieved using an iterative method. Results show that the increase in tensile hoop stress resulted from creep progress must be considered in design progress. In addition, the effect of hygrothermal loading is more extensive after creep evolution.

Keywords: Magneto-electro-elastic (MEE); Time-dependent creep; Thick-walled sphere; Hygrothermal analysis.

1 INTRODUCTION

OWING to the enormous usages of intelligent materials in modern technology, MEE intelligent structures are todays broadly employed in engineering areas. In composites containing piezoelectric materials in addition to piezomagnetic materials, there is an intense magneto-electrical coupling that there is not in a piezoelectric or piezomagnetic material individually. Moreover, MEEs has some superior properties such as the piezoelectric, piezomagnetic and magnetoelectric effects wherein the elastic deformations can be produced by applying an electric or magnetic field as well as mechanical load. Since the intelligent materials are used subjected to different loadings and boundary conditions, disclosing the influences of the humidity, thermal field, magnetic field, electric field and

*Corresponding author.
E-mail address: m.saadatfar@qom.ac.ir (M. Saadatfar).

mechanical field on the performance of them is vital [1-3]. Also, to have the best performance and reliability, creep analysis is valuable for actuators employed for high-precision positioning and load-bearing usages [4]. With the purpose of multiphysical analysis, many researchers tried to explore the multiphysical response of intelligent structures. The coupled hygrothermal analysis of laminated piezoelectric plates is carried out by Smittakorn and Heyliger [5]. Also, they [6] revealed the influence of the hygrothermal as well as electro-mechanical conditions on the static and dynamic response of plates made of adaptive wood composite. Raja et al. [7] studied the stresses in laminated piezoelectric plates and shells under hygrothermal condition. Dai and Wang [8] analytically solved the thermo-magneto-piezoelectric stress and displacement problem of a hollow cylinder. Akbarzadeh and Chen [9] investigated the static behavior of a long hollow smart cylinder under hygrothermal loading. Multiphysical behavior of a functionally graded rotating thick-walled cylinder is studied by Akbarzadeh and Chen [10]. Saadatfar and Aghaie-Khafri [11,12] revealed that the actuation and sensing authority of functionally graded piezoelectric material (FGPM) layers extensively affected by the grading-index of them under hygrothermal loading. Using differential quadrature method (DQM), Saadatfar and Aghaie-Khafri [13] analyzed the response of a functionally graded material (FGM) cylindrical shell integrated with FGPM layers in hygro-thermo-magnetic environmental condition.

The behavior of MEE spherical structures is studied by some researchers. Wang and Ding [14, 15] investigated the dynamic behavior of MEE hollow sphere. Transient thermal stress in a multilayered MEE thick-walled sphere is studied by Ootao and Ishihara [16]. Chen et al [17] investigated the static behavior of an anisotropic and multilayered MEE thick-walled sphere analytically. Saadatfar and Aghaie-Khafri [18] analyzed the Static stresses and displacement in a functionally graded MEE hollow sphere in hygrothermal environmental condition. Investigating the creep behavior of smart piezoelectric spheres is the subject of few articles in the literature. Dai et al. [19] studied the creep behavior in a FGPM sphere subjected to thermo-electro-mechanical loads. Ghorbanpour Arani et al. [20] investigated creep stresses and electric potential redistribution in a piezoelectric thick-walled sphere employing Mendelson's method. Jabbari and Tayebi [21] derived a solution for time-dependent creep problem of a thick-walled sphere made of fluid-saturated porous FGPM placed in a constant magnetic field. Using Burgers' creep model, Loghman and Tourang [22] analyzed the non-stationary creep behavior of a polyvinylidene fluoride (PVDF) smart hollow sphere.

Searching the literature in the area of creep analyses of smart materials shows that there is no published work studying time-dependent creep stress redistribution of a MEE hollow sphere with hygrothermal gradient. This paper makes the first attempt to study the creep behavior of MEE hollow sphere using the Prandtl-Reuss equations and Norton's law. The goal of this research is to explore the effects of conceivable interactions of various physical fields on the response of MEE intelligent materials.

2 THEORETICAL FORMULATIONS

Consider a MEE thick-walled sphere which radially polarized and magnetized in which the interior and exterior radius are a and b, respectively. Concerning spherically symmetric, nonzero components of temperature (T), displacement (u), magnetic potential (ψ), electric potential (Φ) and moisture concentration (M) are function of radius. In the following sections, c_{ij} ,e_{1j} ,q_{1j} ,β_{11}, ε_{11}, d_{11}, p_1, m_1, $\alpha_{i,}$ k^T, k^C, χ_1, γ_1, β_i are the elastic, piezoelectric, piezomagnetic, dielectric, electromagnetic, magnetic, pyroelectric, pyromagnetic, thermal expansion, thermal conductivity, moisture diffusivity, hygroelectric, hygromagnetic and moisture expansion coefficients, respectively.

2.1 Basic equations of problem

The complete strains are supposed to be sum of magnetic, electrical, hygrothermal, mechanical and creep strains. Therefore, the stress-strain relation can be expressed as [18, 19]:

$$\sigma_r = c_{11}\frac{\partial u}{\partial r} + 2c_{12}\frac{u}{r} + e_{11}\frac{\partial \phi}{\partial r} + q_{11}\frac{\partial \psi}{\partial r} - \lambda_1 T - \zeta_1 M - c_{11}\varepsilon_r^c - 2c_{12}\varepsilon_\theta^c \tag{1a}$$

$$\sigma_\theta = c_{12}\frac{\partial u}{\partial r} + (c_{22}+c_{23})\frac{u}{r} + e_{12}\frac{\partial \phi}{\partial r} + q_{12}\frac{\partial \psi}{\partial r} - \lambda_2 T - \zeta_2 M - c_{12}\varepsilon_r^c - (c_{22}+c_{23})\varepsilon_\theta^c, \tag{1b}$$

$$D_r = e_{11}\frac{\partial u}{\partial r} + 2e_{12}\frac{u}{r} - \beta_{11}\frac{\partial \phi}{\partial r} - \varepsilon_{11}\frac{\partial \psi}{\partial r} + p_1 T + \chi_1 M - e_{11}\varepsilon_r^c - 2e_{12}\varepsilon_\theta^c, \tag{1c}$$

$$B_r = q_{11}\frac{\partial u}{\partial r} + 2q_{12}\frac{u}{r} - \varepsilon_{11}\frac{\partial \phi}{\partial r} - d_{11}\frac{\partial \psi}{\partial r} + m_1 T + \gamma_1 M - q_{11}\varepsilon_r^c - 2q_{12}\varepsilon_\theta^c \tag{1d}$$

where, σ_i and ε_i^c ($i = r, \theta$) are stresses and creep strains, respectively. Besides, we have [18, 23]:

$$\lambda_1 = c_{11}\alpha_r + 2c_{12}\alpha_\theta, \qquad \lambda_2 = c_{12}\alpha_r + (c_{22} + c_{23})\alpha_\theta, \tag{2a}$$

$$\zeta_1 = c_{11}\beta_r + 2c_{12}\beta_\theta, \qquad \zeta_2 = c_{12}\beta_r + (c_{22} + c_{23})\beta_\theta, \tag{2b}$$

In the absence of body forces, electric charge and electric current densities, the equations of equilibrium, electrostatics and magnetostatics for MEE sphere can be written as:

$$\frac{\partial \sigma_r}{\partial r} + \frac{2(\sigma_r - \sigma_\theta)}{r} = 0. \tag{3}$$

$$\frac{\partial D_r}{\partial r} + \frac{2D_r}{r} = 0, \tag{4a}$$

$$\frac{\partial B_r}{\partial r} + \frac{2B_r}{r} = 0. \tag{4b}$$

where D_r is the electric displacement and B_r is the magnetic induction. The sphere is considered to be subjected to magneto-electro-mechanical loading. Thus, the boundary conditions can be expressed as follow:

$$\begin{aligned} &\sigma_r\big|_{r=a} = -p_a, \qquad \sigma_r\big|_{r=b} = -p_b, \\ &\phi\big|_{r=a} = \phi_a, \qquad \phi\big|_{r=b} = \phi_b, \\ &\psi\big|_{r=a} = \psi_a, \qquad \psi\big|_{r=b} = \psi_b. \end{aligned} \tag{5}$$

Solving Eqs. (4), gives:

$$D_r = \frac{A_1}{r^2}, \tag{6a}$$

$$B_r = \frac{A_2}{r^2}, \tag{6b}$$

where, A_1 and A_2 are unknown constants. Substituting Eqs. (6) into Eqs. (1c) and (1d), yields:

$$\frac{\partial \phi(r)}{\partial r} = \frac{1}{\beta_{11}}\left(e_{11}\frac{\partial u}{\partial r} + 2e_{12}\frac{u}{r} - \varepsilon_{11}\frac{\partial \psi}{\partial r} - \frac{A_1}{r^2} + p_1 T + \chi_1 M - e_{11}\varepsilon_r^c - 2e_{12}\varepsilon_\theta^c\right) \tag{7a}$$

$$\frac{\partial \psi(r)}{\partial r} = \frac{1}{d_{11}}\left(q_{11}\frac{\partial u}{\partial r} + 2q_{12}\frac{u}{r} - \varepsilon_{11}\frac{\partial \phi}{\partial r} - \frac{A_2}{r^2} + m_1 T + \gamma_1 M - q_{11}\varepsilon_r^c - 2q_{12}\varepsilon_\theta^c\right) \tag{7b}$$

These equations can be rearranged as:

$$\frac{\partial \phi(r)}{\partial r}=\left(L_1\frac{\partial u}{\partial r}+2L_2\frac{u}{r}+L_3\frac{A_2}{r^2}+L_4T+L_6M-L_5\frac{A_1}{r^2}-L_1\varepsilon_r^c-2L_2\varepsilon_\theta^c\right) \tag{8a}$$

$$\frac{\partial \psi(r)}{\partial r}=\left(P_1\frac{\partial u}{\partial r}+2P_2\frac{u}{r}+P_3\frac{A_1}{r^2}+P_4T+P_6M-P_5\frac{A_2}{r^2}-P_1\varepsilon_r^c-2P_2\varepsilon_\theta^c\right) \tag{8b}$$

where,

$$\begin{aligned}
&L_1=\frac{e_{11}d_{11}-\varepsilon_{11}q_{11}}{\beta_{11}d_{11}-\varepsilon_{11}^2},\quad L_2=\frac{e_{12}d_{11}-\varepsilon_{11}q_{12}}{\beta_{11}d_{11}-\varepsilon_{11}^2},\quad L_3=\frac{\varepsilon_{11}}{\beta_{11}d_{11}-\varepsilon_{11}^2},\quad L_4=\frac{d_{11}p_1-\varepsilon_{11}m_1}{\beta_{11}d_{11}-\varepsilon_{11}^2},\\
&L_5=\frac{d_{11}}{\beta_{11}d_{11}-\varepsilon_{11}^2},\quad L_6=\frac{d_{11}\chi_1-\varepsilon_{11}\gamma_1}{\beta_{11}d_{11}-\varepsilon_{11}^2},\quad P_1=\frac{q_{11}\beta_{11}-\varepsilon_{11}e_{11}}{\beta_{11}d_{11}-\varepsilon_{11}^2},\quad P_2=\frac{q_{12}\beta_{11}-e_{12}\varepsilon_{11}}{\beta_{11}d_{11}-\varepsilon_{11}^2},\\
&P_3=\frac{\varepsilon_{11}}{\beta_{11}d_{11}-\varepsilon_{11}^2},\quad P_4=\frac{\beta_{11}m_1-\varepsilon_{11}p_1}{\beta_{11}d_{11}-\varepsilon_{11}^2},\quad P_5=\frac{\beta_{11}}{\beta_{11}d_{11}-\varepsilon_{11}^2},\quad P_6=\frac{\beta_{11}\gamma_1-\varepsilon_{11}\chi_1}{\beta_{11}d_{11}-\varepsilon_{11}^2},
\end{aligned} \tag{9}$$

Substituting Eqs. (8) into Eqs. (1a) and (1b) gives:

$$\sigma_r=C_1\frac{\partial u}{\partial r}+2C_2\frac{u}{r}+C_3\frac{A_2}{r^2}+C_4\frac{A_1}{r^2}+C_5T+C_6M-\lambda_1T-\zeta_1M-C_1\varepsilon_r^c-2C_2\varepsilon_\theta^c, \tag{10a}$$

$$\sigma_\theta=E_1\frac{\partial u}{\partial r}+2E_2\frac{u}{r}+E_3\frac{A_2}{r^2}+E_4\frac{A_1}{r^2}+E_5T+E_6M-\lambda_2T-\zeta_2M-E_1\varepsilon_r^c-2E_1\varepsilon_\theta^c, \tag{10b}$$

where,

$$\begin{aligned}
&C_1=c_{11}+e_{11}L_1+q_{11}P_1,\quad C_2=c_{12}+e_{11}L_2+q_{11}P_2,\quad C_3=e_{11}L_3-q_{11}P_5,\quad C_4=-e_{11}L_5+q_{11}P_3,\\
&C_5=e_{11}L_4+q_{11}P_4,\quad C_6=e_{11}L_6+q_{11}P_6,\quad E_1=c_{12}+e_{12}L_1+q_{12}P_1,\quad E_2=(\frac{c_{22}+c_{23}}{2})+e_{12}L_2+q_{12}P_2,\\
&E_3=e_{12}L_3-q_{12}P_5,\quad E_4=-e_{12}L_5+q_{12}P_3,\quad E_5=e_{12}L_4+q_{12}P_4,\quad E_6=e_{12}L_6+q_{12}P_6
\end{aligned} \tag{11}$$

Substituting Eqs. (10) into Eq. (3), the equilibrium equation can be rewritten as:

$$\begin{aligned}
&\frac{\partial^2u}{\partial r^2}+\frac{1}{r}M_1\frac{\partial u}{\partial r}+\frac{1}{r^2}M_2u=\left(M_3+M_4\right)\frac{T}{r}+\left(-M_5+M_6\right)\frac{\partial T}{\partial r}+M_7\frac{A_2}{r^3}+M_8\frac{A_1}{r^3}+\left(M_9+M_{10}\right)\frac{M}{r}\\
&+\left(-M_{11}+M_{12}\right)\frac{\partial M}{\partial r}+M_{13}r^{-1}\varepsilon_r^c+\frac{\partial \varepsilon_r^c}{\partial r}+2M_{14}r^{-1}\varepsilon_\theta^c+2M_{15}\frac{\partial \varepsilon_\theta^c}{\partial r}
\end{aligned} \tag{12}$$

where,

$$\begin{aligned}
&M_1=\frac{2C_1+2C_2-2E_1}{C_1},\quad M_2=\frac{2C_2-4E_2}{C_1},\quad M_3=\frac{2\left(-2\lambda_1+\lambda_2\right)}{C_1},\quad M_4=\frac{2E_5-2C_5}{C_1},\quad M_5=\frac{C_5}{C_1},\\
&M_6=\frac{\lambda_1}{C_1},\quad M_7=\frac{2E_3}{C_1},\quad M_8=\frac{2E_4}{C_1},\quad M_9=\frac{2\left(-2\zeta_1+\zeta_2\right)}{C_1},\quad M_{10}=\frac{2E_6-2C_6}{C_1},\quad M_{11}=\frac{C_6}{C_1},\\
&M_{12}=\frac{\zeta_1}{C_1},\quad M_{13}=\frac{2C_1-2E_1}{C_1},\quad M_{14}=\frac{2C_2-2E_2}{C_1},\quad M_{15}=\frac{C_2}{C_1}
\end{aligned} \tag{13}$$

For solving the Eq. (12), the temperature and moisture concentration functions must be found.

2.2 Temperature and moisture concentration distribution

In an uncoupled hygrothermal problem, the heat conduction equation and moisture diffusion equation can be solved independently. The uncoupled steady-state axisymmetric heat conduction and Fickian moisture diffusion equations are expressed as [18]:

$$\frac{1}{r^2}\frac{\partial}{\partial r}(r^2 k^T \frac{\partial T}{\partial r}) = 0, \tag{14a}$$

$$\frac{1}{r^2}\frac{\partial}{\partial r}(r^2 k^C \frac{\partial M}{\partial r}) = 0, \tag{14b}$$

Integrating Eqs. (14) twice gives:

$$\begin{aligned} T(r) &= W_1 r^{-1} + W_2, \\ M(r) &= S_1 r^{-1} + S_2. \end{aligned} \tag{15}$$

where, W_i and S_i (i=1, 2) are unknown constant. The moisture concentration change M_a and M_b and temperatures change T_a and T_b are assumed at the inner and outer surfaces of the sphere, respectively. Utilizing these boundary conditions, W_i and S_i are achieved as:

$$W_1 = \frac{T_a - T_b}{a^{-1} - b^{-1}}, \qquad W_2 = \frac{-T_a b^{-1} + T_b a^{-1}}{a^{-1} - b^{-1}}, \tag{16a}$$

$$S_1 = \frac{M_a - M_b}{a^{-1} - b^{-1}}, \qquad S_2 = \frac{-M_a b^{-1} + M_b a^{-1}}{a^{-1} - b^{-1}}. \tag{16b}$$

2.3 Primitive hygrothermal analysis of the MEE thick-walled sphere

In primitive state, eliminating creep strains in Eq. (12) yields:

$$\begin{aligned} &\frac{\partial^2 u}{\partial r^2} + \frac{M_1}{r}\frac{\partial u}{\partial r} + \frac{M_2}{r^2}u = \frac{(M_3 W_2 + M_9 S_2 + M_4 W_2 + M_{10} S_2)}{r} + \frac{\left[W_1(M_4 + M_5) + S_1(M_{10} + M_{11})\right]}{r^2} \\ &+ \frac{\left[W_1(M_3 - M_6) + S_1(M_9 - M_{12})\right]}{r^2} + M_7 \frac{A_2}{r^3} + M_8 \frac{A_1}{r^3}. \end{aligned} \tag{17}$$

The complete solution of Eq. (17) can be considered as:

$$u = u_g + u_p. \tag{18}$$

Concerning the homogeneous solution, for the numerical values to be used, only real distinct roots will be found [18]. So, the homogeneous solution of the Eq. (17) is expressed as:

$$u_g = B_1 r^{m_1} + B_2 r^{m_2}, \tag{19a}$$

$$m_{1,2} = \frac{1}{2}\left(-(M_1 - 1) \pm \sqrt{(M_1 - 1)^2 - 4M_2}\right) \tag{19b}$$

where, B_1 and B_2 are unknown constants. Also, the particular solution can be considered as:

$$u_p = B_3 r + B_4 + B_5 A_2 r^{-1} + B_6 A_1 r^{-1}, \tag{20}$$

where,

$$B_3 = \frac{(M_4 + M_3)W_2 + (M_{10} + M_9)S_2}{M_1 + M_2},\ B_4 = \frac{W_1(M_4 + M_5 + M_3 - M_6) + S_1(M_{10} + M_{11} + M_9 - M_{12})}{M_2},$$
$$B_5 = \frac{M_7}{2 - M_1 + M_2}, \qquad B_6 = \frac{M_8}{2 - M_1 + M_2}. \tag{21}$$

Utilizing Eqs. (19) and (20) we have:

$$u = u_g + u_p = B_1 r^{m_1} + B_2 r^{m_2} + B_3 r + B_4 + B_5 A_2 r^{-1} + B_6 A_1 r^{-1}. \tag{22}$$

Now, using Eq. (22), Eq. (8a) can be written as:

$$\frac{\partial \phi(r)}{\partial r} = \left(L_1\left(B_1 m_1 r^{m_1 - 1} + B_2 m_2 r^{m_2 - 1} + B_3 - B_5 A_2 r^{-2} - B_6 A_1 r^{-2}\right)\right) + L_4\left(W_1 r^{-1} + W_2\right) + L_6\left(S_1 r^{-1} + S_2\right)$$
$$+ 2L_2\left(B_1 r^{m_1 - 1} + B_2 r^{m_2 - 1} + B_3 + B_4 r^{-1} + B_5 A_2 r^{-2} + B_6 A_1 r^{-2}\right) + L_3 \frac{A_2}{r^2} - L_5 \frac{A_1}{r^2}. \tag{23}$$

Integrating Eq. (23) gives:

$$\phi(r) = \left(L_1\left(B_1 r^{m_1} + B_2 r^{m_2} + B_3 r + B_5 A_2 r^{-1} + B_6 A_1 r^{-1}\right)\right) + L_4\left(W_1 \ln(\mathrm{r}) + W_2 r\right) + L_6\left(S_1 \ln(\mathrm{r}) + S_2 r\right)$$
$$+ 2L_2\left(\frac{B_1}{m_1} r^{m_1} + \frac{B_2}{m_2} r^{m_2} + B_3 r + B_4 \ln(\mathrm{r}) - B_5 A_2 r^{-1} - B_6 A_1 r^{-1}\right) - L_3 A_2 r^{-1} + L_5 A_1 r^{-1} + Z_1. \tag{24}$$

where Z_1 is an unknown constant. In a similar way, $\psi(r)$ is achieved as:

$$\psi(r) = \left(P_1\left(B_1 r^{m_1} + B_2 r^{m_2} + B_3 r + B_5 A_2 r^{-1} + B_6 A_1 r^{-1}\right)\right) + P_4\left(W_1 \ln(\mathrm{r}) + W_2 r\right) + P_6\left(S_1 \ln(\mathrm{r}) + S_2 r\right)$$
$$+ 2P_2\left(\frac{B_1}{m_1} r^{m_1} + \frac{B_2}{m_2} r^{m_2} + B_3 r + B_4 \ln(\mathrm{r}) - B_5 A_2 r^{-1} - B_6 A_1 r^{-1}\right) + P_5 A_2 r^{-1} - P_3 A_1 r^{-1} + Z_2. \tag{25}$$

where Z_2 is an unknown constant. Using Eqs. (24) and (25) into Eqs. (10), the radial and hoop stresses are achieved as:

$$\sigma_r = C_1\left(B_1 m_1 r^{m_1 - 1} + B_2 m_2 r^{m_2 - 1} + B_3 - B_5 A_2 r^{-2} - B_6 A_1 r^{-2}\right) + \left(C_5 - \lambda_1\right)\left(W_1 r^{-1} + W_2\right) + \left(C_6 - \zeta_1\right)\left(S_1 r^{-1} + S_2\right)$$
$$+ 2C_2\left(B_1 r^{m_1 - 1} + B_2 r^{m_2 - 1} + B_3 + B_4 r^{-1} + B_5 A_2 r^{-2} + B_6 A_1 r^{-2}\right) + C_3 \frac{A_2}{r^2} + C_4 \frac{A_1}{r^2}. \tag{26}$$

$$\sigma_\theta = E_1\left(B_1 m_1 r^{m_1 - 1} + B_2 m_2 r^{m_2 - 1} + B_3 - B_5 A_2 r^{-2} - B_6 A_1 r^{-2}\right) + \left(E_5 - \lambda_2\right)\left(W_1 r^{-1} + W_2\right) + \left(E_6 - \zeta_2\right)\left(S_1 r^{-1} + S_2\right)$$
$$+ 2E_2\left(B_1 r^{m_1 - 1} + B_2 r^{m_2 - 1} + B_3 + B_4 r^{-1} + B_5 A_2 r^{-2} + B_6 A_1 r^{-2}\right) + E_3 \frac{A_2}{r^2} + E_4 \frac{A_1}{r^2}. \tag{27}$$

Using the magneto-electro-mechanical boundary conditions, the unknown constants A_1, A_2, B_1, B_2, Z_1 and Z_2 can be determined by solving a system of six linear algebraic equations. The system of six linear algebraic equations can be considered in the following form:

$$X\begin{bmatrix} B_1 & B_2 & A_1 & A_2 & Z_1 & Z_2 \end{bmatrix}^T = F, \tag{28}$$

where:

$$\begin{aligned}
X_1 &= \begin{bmatrix} (C_1 m_1 + 2C_2)a^{m_1-1} & (C_1 m_2 + 2C_2)a^{m_1-1} & a^{-2}(C_4 - C_1 B_6 + 2C_2 B_6) & a^{-2}(C_3 - C_1 B_5 + 2C_2 B_5) & 0 & 0 \end{bmatrix} \\
X_2 &= \begin{bmatrix} (m_1 C_1 + 2C_2)b^{m_1-1} & (m_2 C_1 + 2C_2)b^{m_2-1} & b^{-2}(B_6(2C_2 - C_1) + C_4) & b^{-2}(B_5(2C_2 - C_1) + C_3) & 0 & 0 \end{bmatrix} \\
X_3 &= \begin{bmatrix} a^{m_1}(2L_2 m_1^{-1} + L_1) & a^{m_2}(2L_2 m_2^{-1} + L_1) & a^{-1}(L_5 - 2L_2 B_6 + L_1 B_6) & a^{-1}(-L_3 - 2L_2 B_5 + L_1 B_5) & 1 & 0 \end{bmatrix} \\
X_4 &= \begin{bmatrix} b^{m_1}(2L_2 m_1^{-1} + L_1) & b^{m_2}(2L_2 m_2^{-1} + L_1) & b^{-1}(L_5 - 2L_2 B_6 + L_1 B_6) & b^{-1}(-L_3 - 2L_2 B_5 + L_1 B_5) & 1 & 0 \end{bmatrix} \\
X_5 &= \begin{bmatrix} a^{m_1}(P_1 + 2P_2 m_1^{-1}) & a^{m_2}(P_1 + 2P_2 m_2^{-1}) & a^{-1}(P_1 B_6 - 2P_2 B_6 - P_3) & a^{-1}(B_5 P_1 - 2P_2 B_5 + P_5) & 0 & 1 \end{bmatrix} \\
X_6 &= \begin{bmatrix} b^{m_1}(P_1 + 2P_2 m_1^{-1}) & b^{m_2}(P_1 + 2P_2 m_2^{-1}) & b^{-1}(P_1 B_6 - 2P_2 B_6 - P_3) & b^{-1}(B_5 P_1 - 2P_2 B_5 + P_5) & 0 & 1 \end{bmatrix} \\
F &= \begin{bmatrix} P_a - S_1|_{r=a} & P_b - S_1|_{r=b} & \phi_a - S_2|_{r=a} & \phi_b - S_2|_{r=b} & \psi_a - S_3|_{r=a} & \psi_b - S_3|_{r=b} \end{bmatrix}^{-1} \\
S_1 &= B_3(C_1 + 2C_2) + 2C_2 B_4 r^{-1} + (C_5 - \lambda_1)(W_1 a^{-1} + W_2) + (C_6 - \zeta_1)(S_1 r^{-1} + S_2) \\
S_2 &= (L_1 + 2L_2)B_3 r + 2L_2 B_4 \ln(r) + L_4(W_1 \ln(r) + W_2 r) + L_6(S_1 \ln(r) + S_2 r) \\
S_3 &= (P_1 + 2P_2)B_3 r + 2P_2 B_4 \ln(r) + P_4(W_1 \ln(r) + W_2 r) + P_6(S_1 \ln(r) + S_2 r)
\end{aligned} \tag{29}$$

By solving the Eq. (28), the radial displacement as well as electric potential, stresses and magnetic potential are achieved at zero time.

2.4 Creep analysis of MEE thick-walled sphere

Assuming the hygrothermal field to be steady-state, differentiation Eq. (12) with respect to time yields:

$$\frac{\partial^2 \dot{u}}{\partial r^2} + \frac{1}{r} M_1 \frac{\partial \dot{u}}{\partial r} + \frac{1}{r^2} M_2 \dot{u} = M_7 \frac{\dot{A}_2}{r^3} + M_8 \frac{\dot{A}_1}{r^3} + M_{13} r^{-1} \dot{\varepsilon}_r^c + \frac{\partial \dot{\varepsilon}_r^c}{\partial r} + 2M_{14} r^{-1} \dot{\varepsilon}_\theta^c + 2M_{15} \frac{\partial \dot{\varepsilon}_\theta^c}{\partial r} \tag{30}$$

The relation between creep rates and the stresses are expressed by the famous Prandtl-Reuss equations as the following form [24]:

$$\begin{aligned}
\dot{\varepsilon}_r^c &= \dot{\varepsilon}_e^c \sigma_e^{-1}\left(\sigma_r - 0.5(\sigma_\theta + \sigma_\phi)\right) \\
\dot{\varepsilon}_\theta^c &= \dot{\varepsilon}_e^c \sigma_e^{-1}\left(\sigma_\theta - 0.5(\sigma_r + \sigma_\phi)\right) \\
\dot{\varepsilon}_\phi^c &= \dot{\varepsilon}_e^c \sigma_e^{-1}\left(\sigma_\phi - 0.5(\sigma_\theta + \sigma_r)\right)
\end{aligned} \tag{31}$$

where $\dot{\varepsilon}_i^c (\mathrm{i} = \mathrm{r}, \theta, \phi)$, $\dot{\varepsilon}_e^c$ and σ_e are the creep strain rate, effective creep strain rate and the effective stress, respectively. Norton's law is considered as the creep constitutive model as [25]:

$$\dot{\varepsilon}_e^c = B(\mathrm{r})\sigma_e^{n(\mathrm{r})} \tag{32}$$

where material creep parameters $B(r)$ and $n(r)$ are function of radius as:

$$B(\mathrm{r}) = b_0 r^{b_1},\ n(\mathrm{r}) = n_0 \tag{33}$$

where b_0,b_1 and n_0 are constants. Considering the axisymmetric of the sphere and using Eq. (32) into Eqs. (31), gives:

$$\begin{aligned}\dot{\varepsilon}_r^c &= -B(\mathrm{r})\sigma_e^{n_0-1}\left(\sigma_\theta-\sigma_r\right)\\ \dot{\varepsilon}_\theta^c &= 0.5B(\mathrm{r})\sigma_e^{n_0-1}\left(\sigma_\theta-\sigma_r\right)\end{aligned} \tag{34}$$

Using the Von Mises equivalent stress, we have:

$$\sigma_e=\frac{1}{\sqrt{2}}\sqrt{(\sigma_\theta-\sigma_r)^2+(\sigma_\theta-\sigma_\phi)^2+(\sigma_\phi-\sigma_r)^2}=\left|\sigma_\theta-\sigma_r\right| \tag{35}$$

Eqs. (34) are rewritten as:

$$\begin{aligned}\dot{\varepsilon}_r^c &= -B(\mathrm{r})\sigma_e^{n_0}\\ \dot{\varepsilon}_\theta^c &= 0.5B(\mathrm{r})\sigma_e^{n_0}\end{aligned} \tag{36}$$

Substituting Eq. (36) into Eq. (30), we have:

$$\frac{\partial^2\dot{u}}{\partial r^2}+\frac{1}{r}M_1\frac{\partial\dot{u}}{\partial r}+\frac{1}{r^2}M_2\dot{u}=M_7\frac{\dot{A}_2}{r^3}+M_8\frac{\dot{A}_1}{r^3}+b_0r^{b_1-1}\sigma_e^{n_0}\left(M_{14}+M_{15}b_1-M_{13}-b_1\right)+\left(M_{15}-1\right)b_0r^{b_1}\frac{\partial\sigma_e^{n_0}}{\partial r} \tag{37}$$

By the same way as in previous section, the solution is:

$$\dot{u}=D_1r^{m_1}+D_2r^{m_2}+G_{11}r^{m_1}+G_{21}r^{m_2}+B_6r^{-1}\dot{A}_1+B_5r^{-1}\dot{A}_2 \tag{38}$$

where D_1 and D_2 are constant and $G_{11}(r)$ and $G_{21}(r)$ can be determined using the method of variation of parameters as [26]:

$$\begin{aligned}G_{11}(\mathrm{r}) &= \frac{b_0}{m_2-m_1}\int\left\{r^{b_1-m_1}\sigma_e^{n_0}\left(M_{14}+M_{15}b_1-M_{13}-b_1\right)+\left(M_{15}-1\right)r^{b_1-m_1+1}\frac{\partial\sigma_e^{n_0}}{\partial r}\right\}dr\\ G_{21}(\mathrm{r}) &= -\frac{b_0}{m_2-m_1}\int\left\{r^{b_1-m_2}\sigma_e^{n_0}\left(M_{14}+M_{15}b_1-M_{13}-b_1\right)+\left(M_{15}-1\right)r^{b_1-m_2+1}\frac{\partial\sigma_e^{n_0}}{\partial r}\right\}dr\end{aligned} \tag{39}$$

Differentiation Eqs. (8) and (10) with respect to time yields:

$$\dot{\sigma}_r=C_1\frac{\partial\dot{u}}{\partial r}+2C_2\frac{\dot{u}}{r}+C_3\frac{\dot{A}_2}{r^2}+C_4\frac{\dot{A}_1}{r^2}+\left(C_1-C_2\right)b_0r^{b_1}\sigma_e^{n_0}, \tag{40a}$$

$$\dot{\sigma}_\theta=E_1\frac{\partial\dot{u}}{\partial r}+2E_2\frac{\dot{u}}{r}+E_3\frac{\dot{A}_2}{r^2}+E_4\frac{\dot{A}_1}{r^2}+\left(E_1-E_2\right)b_0r^{b_1}\sigma_e^{n_0}, \tag{40b}$$

$$\frac{\partial\dot{\phi}}{\partial r}=L_1\frac{\partial\dot{u}}{\partial r}+2L_2\frac{\dot{u}}{r}-L_5\frac{\dot{A}_1}{r^2}+L_3\frac{\dot{A}_2}{r^2}-L_1\dot{\varepsilon}_r^c-2L_2\dot{\varepsilon}_\theta^c \tag{40c}$$

$$\frac{\partial\dot{\psi}}{\partial r}=P_1\frac{\partial\dot{u}}{\partial r}+2P_2\frac{\dot{u}}{r}+P_3\frac{\dot{A}_1}{r^2}-P_5\frac{\dot{A}_2}{r^2}-P_1\dot{\varepsilon}_r^c-2P_2\dot{\varepsilon}_\theta^c \tag{40d}$$

Substituting Eq. (38) into Eqs. (40) and integrating Eqs. (40c) and (40d), after rearranging, gives:

$$\dot{\sigma}_r = D_1\left(\left(m_1C_1+2C_2\right)r^{m_1-1}\right)+D_2\left(\left(m_2C_1+2C_2\right)r^{m_2-1}\right)+\left(B_6\left(2C_2-C_1\right)+C_4\right)\frac{\dot{A}_1}{r^2}+\left(B_5\left(2C_2-C_1\right)+C_3\right)\frac{\dot{A}_2}{r^2}$$
$$+C_1\left(\frac{\partial G_{11}}{\partial r}r^{m_1}+G_{11}m_1r^{m_1-1}+\frac{\partial G_{21}}{\partial r}r^{m_2}+G_{21}m_2r^{m_2-1}\right)+2C_2r^{-1}\left(G_{11}r^{m_1}+G_{21}r^{m_2}\right)+\left(C_1-C_2\right)b_0r^{b_1}\sigma_e^{n_0} \quad (41a)$$

$$\dot{\sigma}_\theta = D_1\left(\left(m_1E_1+2E_2\right)r^{m_1-1}\right)+D_2\left(\left(m_2E_1+2E_2\right)r^{m_2-1}\right)+\left(B_6\left(2E_2-E_1\right)+E_4\right)\frac{\dot{A}_1}{r^2}+\left(B_5\left(2E_2-E_1\right)+E_3\right)\frac{\dot{A}_2}{r^2}$$
$$+E_1\left(\frac{\partial G_{11}}{\partial r}r^{m_1}+G_{11}m_1r^{m_1-1}+\frac{\partial G_{21}}{\partial r}r^{m_2}+G_{21}m_2r^{m_2-1}\right)+2E_2r^{-1}\left(G_{11}r^{m_1}+G_{21}r^{m_2}\right)+\left(E_1-E_2\right)b_0r^{b_1}\sigma_e^{n_0} \quad (41b)$$

$$\dot{\phi} = D_1r^{m_1}\left(L_1+\frac{2L_2}{m_1}\right)+D_2r^{m_2}\left(L_1+\frac{2L_2}{m_2}\right)-\left(B_6\left(2L_2-L_1\right)-L_5\right)\dot{A}_1r^{-1}-\left(B_5\left(2L_2-L_1\right)+L_3\right)\dot{A}_2r^{-1}+J_1$$
$$+\int\left(L_1\left(\frac{\partial G_{11}}{\partial r}r^{m_1}+G_{11}m_1r^{m_1-1}+\frac{\partial G_{21}}{\partial r}r^{m_2}+G_{21}m_2r^{m_2-1}\right)+2L_2\left(+G_{11}r^{m_1-1}+G_{21}r^{m_2-1}\right)+\left(L_1-L_2\right)b_0r^{b_1}\sigma_e^{n_0}\right)dr \quad (41c)$$

$$\dot{\psi} = D_1r^{m_1}\left(P_1+\frac{2P_2}{m_1}\right)+D_2r^{m_2}\left(P_1+\frac{2P_2}{m_2}\right)-\left(B_6\left(2P_2-P_1\right)+P_3\right)r^{-1}\dot{A}_1-\left(B_5\left(2P_2-P_1\right)-P_5\right)\dot{A}_2r^{-1}+J_2$$
$$+\int\left(P_1\left(\frac{\partial G_{11}}{\partial r}r^{m_1}+G_{11}m_1r^{m_1-1}+\frac{\partial G_{21}}{\partial r}r^{m_2}+G_{21}m_2r^{m_2-1}\right)+2P_2\left(+G_{11}r^{m_1-1}+G_{21}r^{m_2-1}\right)+\left(P_1-P_2\right)b_0r^{b_1}\sigma_e^{n_0}\right)dr \quad (41d)$$

where J_1 and J_2 are constant. The boundary conditions must be used to determine unknown constants. The mechanical pressures, electric and magnetic potentials of interior and exterior surface of the MEE sphere do not vary over the time, so we have:

$$\begin{aligned}&\dot{\sigma}_r\big|_{r=a}=0, \quad \dot{\sigma}_r\big|_{r=b}=0,\\ &\dot{\phi}\big|_{r=a}=0, \quad \dot{\phi}\big|_{r=b}=0,\\ &\dot{\psi}\big|_{r=a}=0, \quad \dot{\psi}\big|_{r=b}=0.\end{aligned} \quad (42)$$

The resultant system of six linear equations can be solved like as previous section. The components of matrix X are as previous case and the component of matrix F are written as:

$$\begin{aligned}&X\left[D_1 \quad D_2 \quad \dot{A}_1 \quad \dot{A}_2 \quad J_1 \quad J_2\right]^T = F\\ &F = -\left[S_1\big|_{r=a} \quad S_1\big|_{r=b} \quad S_2\big|_{r=a} \quad S_2\big|_{r=b} \quad S_3\big|_{r=a} \quad S_3\big|_{r=b}\right]\\ &S_1 = C_1\left(\frac{\partial G_{11}}{\partial r}r^{m_1}+G_{11}m_1r^{m_1-1}+\frac{\partial G_{21}}{\partial r}r^{m_2}+G_{21}m_2r^{m_2-1}\right)+2C_2r^{-1}\left(G_{11}r^{m_1}+G_{21}r^{m_2}\right)+\left(C_1-C_2\right)b_0r^{b_1}\sigma_e^{n_0}\\ &S_2 = \int\left(L_1\left(\frac{\partial G_{11}}{\partial r}r^{m_1}+G_{11}m_1r^{m_1-1}+\frac{\partial G_{21}}{\partial r}r^{m_2}+G_{21}m_2r^{m_2-1}+2L_2\left(+G_{11}r^{m_1-1}+G_{21}r^{m_2-1}\right)+\left(L_1-L_2\right)b_0r^{b_1}\sigma_e^{n_0}\right)dr\right.\\ &S_3 = \int\left(P_1\left(\frac{\partial G_{11}}{\partial r}r^{m_1}+G_{11}m_1r^{m_1-1}+\frac{\partial G_{21}}{\partial r}r^{m_2}+G_{21}m_2r^{m_2-1}+2P_2\left(+G_{11}r^{m_1-1}+G_{21}r^{m_2-1}\right)+\left(P_1-P_2\right)b_0r^{b_1}\sigma_e^{n_0}\right)dr\right.\end{aligned} \quad (43)$$

2.5 Numerical procedure to achieve history of stresses

To obtain history of stresses in addition to electric and magnetic potential during creep progress, the stress rates and the gradient of electric and magnetic potential are needed. Step-by-step procedure is explained in detail as follows:

1) A suitable time increment should be selected for timing steps. As the creep progress improves in the time, the sum of time steps is total time. After the i_{th} timing step, the total time can be expressed as:

$$t_i = \sum_{k=0}^{i} dt^{(k)} \tag{44}$$

2) Immediately after loading, the creep strains are zero and the solution is an elasticity problem. So, primitive values of stresses, potentials are obtained from Eqs. (26), (27), (24) and (25), respectively. So, the values of stresses in the first time step are acquired.
3) G_{11} and G_{21} are calculated numerically, and then, the stresses and potentials rates for the first step are obtained using Eqs. (41).
4) In the next time steps, the stresses (potentials) and stresses rates (potentials rates) redistributions for previous step are available. So, the stresses (potentials) redistributions are obtained by general formulation of the iterative method:

$$\Sigma^{(i)}(r, t_i) = \Sigma^{(i-1)}(r, t_{i-1}) + \dot{\Sigma}^{(i-1)}(r, t_{i-1})\, dt^{(i)}, \quad \Sigma = \sigma_r, \sigma_\theta, \varphi, \psi \tag{45}$$

5) This iterative procedure is repeated for the total time steps.

3 NUMERICAL RESULTS AND DISCUSSIONS

Here, the creep behavior and effective parameters on the response of the MEE sphere are investigated and discussed comprehensively. Material constants for the material to be used for MEE are listed in Table 1. [18, 19]. The inner radii a=0.1m and outer radii b=0.25m are taken. The following non-dimensional quantities are used for simplicity:

$$R = \frac{r-a}{b-a}, \quad u^* = \frac{u(r)}{a}, \quad \sigma_i^* = \frac{\sigma_i}{P_a}, (i = r, \theta), \quad \phi^* = \sqrt{\frac{\dot{\beta}_{11}}{\dot{c}_{11}}}\frac{\phi(r)}{b}, \quad \psi^* = \sqrt{\frac{\dot{d}_{11}}{\dot{c}_{11}}}\frac{\psi(r)}{b}. \tag{46}$$

First of all, the creep progress during the time is studied. The multiphysical boundary conditions are taken as:

$$P_a = 7MPa, \quad \phi_a = 0, \quad \phi_b = 3000, \ \psi_a = 0, \ \psi_b = 0, \ T_a = 0, \ T_b = 30, \ M_a = 0, \ M_b = 0.25 \tag{47}$$

Fig. 1 demonstrates the creep evolution of hollow MEE sphere under multiphysical environmental condition and loading. In this analysis, the time increment dt=2 hour is used. It is obvious from Fig. 1(a), (e) and (f) that the radial stress, electric potential and magnetic potential have no change with time at the inner and outer radii of the sphere which satisfies the constant electro-magnetic and mechanical boundary conditions. The variations in the rate of stresses, electric and magnetic potentials and displacement, without considering the value, become less extensive during the time. Fig. 1(b) depicts that by serving the time, the positive circumferential stress is decreased at the interior surface (as far as becomes negative) and is increased at the exterior surface with decreasing rate. Besides, by serving the time, the magnitude of maximum hoop stress is rised and its location is moved from the inner radius toward outer radius. This increase in tensile hoop stress must be considered in design progress because the circumferential stress rather than the radial stress is the reason of the failure of elastic thick-walled spheres [23, 27]. According to Fig. 1(c), the equivalent stress is decreased with time at the interior surface, while it exhibits a reverse behavior at the exterior surface. Fig. 1(d) shows that outward maximum radial displacement is at the inner radius and it decreases smoothly toward the external surface. Also, with serving the time, the displacement is rised at a reducing rate. Fig. 1(f) reveals that the absolute value of magnetic potentials, in the same point of radius, is increased with the time at a decreasing rate.

The influence of hygrothermal environmental condition on the initial and creep response of the MEE sphere is disclosed in Fig 2. The temperature and moisture concentration are considered to be zero on the interior surface. However, the moisture concentration and temperature are rised on the exterior surface. In this case, P_a=5 MPa and M_b=T_b/200 are taken and other boundary conditions are as previous case. Concerning Fig. 2(a), rising in hygrothermal loading yields to reduction in compressive radial stress both in initial state and after creep evolution. More enhancement in hygrothermal loading results in tensile radial stress in a part of thickness especially after creep progress. Consequently, for designing purpose, the effect of hygrothermal loading after creep progress is more

important rather than initial state because these ceramics are mechanically brittle and are very sensitive to tensile loads and may not be utilizable after some years. Fig. 2(b) shows that increasing the hygrothermal loading results in rising in both initial and creep hoop stress. Also, there is a fix point near the outer radius for initial circumferential stress and near the inner radius for creep circumferential stress that the hoop stress does not change with a change in hygrothermal loading. In addition, the tensile circumferential stress for the initial state becomes maximum at the inner radius. Conversely, after creep progress, the hoop stress becomes compressive at the inner radius. Fig. 2(c) depicts that rising in applied hygrothermal loading rises both the initial and creep outward radial displacement. This increase is higher after creep progress. Also, after creep progress, the radial displacement becomes maximum at the interior surface. Fig. 2(d) demonstrates that rising in hygrothermal loading results in rising in the electric potential (regardless of the sign) in both the initial and creep case. Fig. 2(e) shows that rising in hygrothermal loading rises the magnetic potential in both initial and creep case.

To reveal the influence of moisture dependence as well as temperature dependence of the elastic coefficients on the response of MEE sphere, the elastic coefficients are presented in the form of [9]:

$$C_{ij} = C_{ij0}(1+\alpha^{*}\,\mathrm{T}+\beta^{*}\,\mathrm{M}) \tag{48}$$

where, C_{ij0} is the elastic coefficient which is independent of temperature and humidity. Also, α^{*} and β^{*} are empirical coefficients for the temperature and humidity dependence, respectively. Here, to have no non-linear equations, it is supposed to rise the temperature and moisture uniformly. So, the sphere is under uniform temperature and moisture concentration increase, T=50, M=0.25 and we have: P_a= 50MPa. Other boundary conditions are kept unchanged. Fig. 3 indicates the influences of the temperature dependence as well as humidity dependence on the initial and creep response of the MEE sphere. Owing to similarity of the influence of the temperature and humidity on the multiphysical behavior, the same magnitudes are considered for the empirical constants, while $\alpha^{*}=\beta^{*}=0$ indicates the material properties which are independent of temperature and moisture. Fig. 3(a) shows that negative value of empirical constants increases both the initial and creep compressive radial stress, whereas the positive value has a reverse effect. Fig. 3(b) depicts that the initial circumferential stress is decreased for minus value of empirical constants while the effect of positive value is reverse. The changes are negligible near the outer radius for the initial stress. Furthermore, it is observed that the effect of empirical constants on the hoop stress after creep progress is negligible. Fig. 3(c) and (d) illustrate that, after creep evolution, negative value of empirical constants leads to an increase in electric and magnetic potential of each point while the positive value has a reverse effect. The changes are more significant after creep evolution. According to Fig. 3(e), minus value of empirical constant rises the outward radial displacement and reversely, the positive value of empirical constant decreases the radial displacement.

To the best of author's knowledge, there is no available paper in the literature for time-dependent creep analysis of MEE spheres. However, static behavior of MEE thick-walled sphere has been studied in Ref. [18]. Thus, to verify the results, the radial and hoop stress distributions is compared in Fig. 4. The details of non-dimensional parameters and material constants can be found in Ref. [18]. In this case: P_a=2KPa, T_b=2, Φ_b=2000 and other boundary condition are kept at zero. As can be seen, due to analytical method, the results have a very good agreement.

Table 1
Material constants.

$c_{11}(GPa)$	$c_{12}\ (GPa)$	$c_{23}\ (GPa)$	$c_{22}\ (GPa)$	$e_{11}\ (C/m^2)$
215	120	120	218	7.5
$e_{12}\ (C/m^2)$	$\alpha_r\ (1/K)$	$\alpha_\theta\ (1/K)$	$q_{11}\ (N/Am)$	$q_{12}\ (N/Am)$
-2.5	6×10^{-6}	15×10^{-6}	345	265
$\beta_{11}(C^2/N\,m^2)$	$d_{11}(Ns^2/C^2)$	$\varepsilon_{11}\ (Ns/VC)$	$\beta_r\ (m^3/kg)$	$\beta_\theta\ (m^3/kg)$
5.8×10^{-9}	95×10^{-6}	2.82×10^{-9}	0.8×10^{-4}	1.2×10^{-4}
$m_1(N/AmK)$	$\chi_1\ (Cm/kg)$	$P_1(C^2/m^2k)$	$\gamma_1\ (Nm^2/Akg)$	n_0
2.5×10^{-5}	0	-2.5×10^{-5}	0	3
b_1	b_0	ρ		
-5	0.11×10^{-36}	7530		

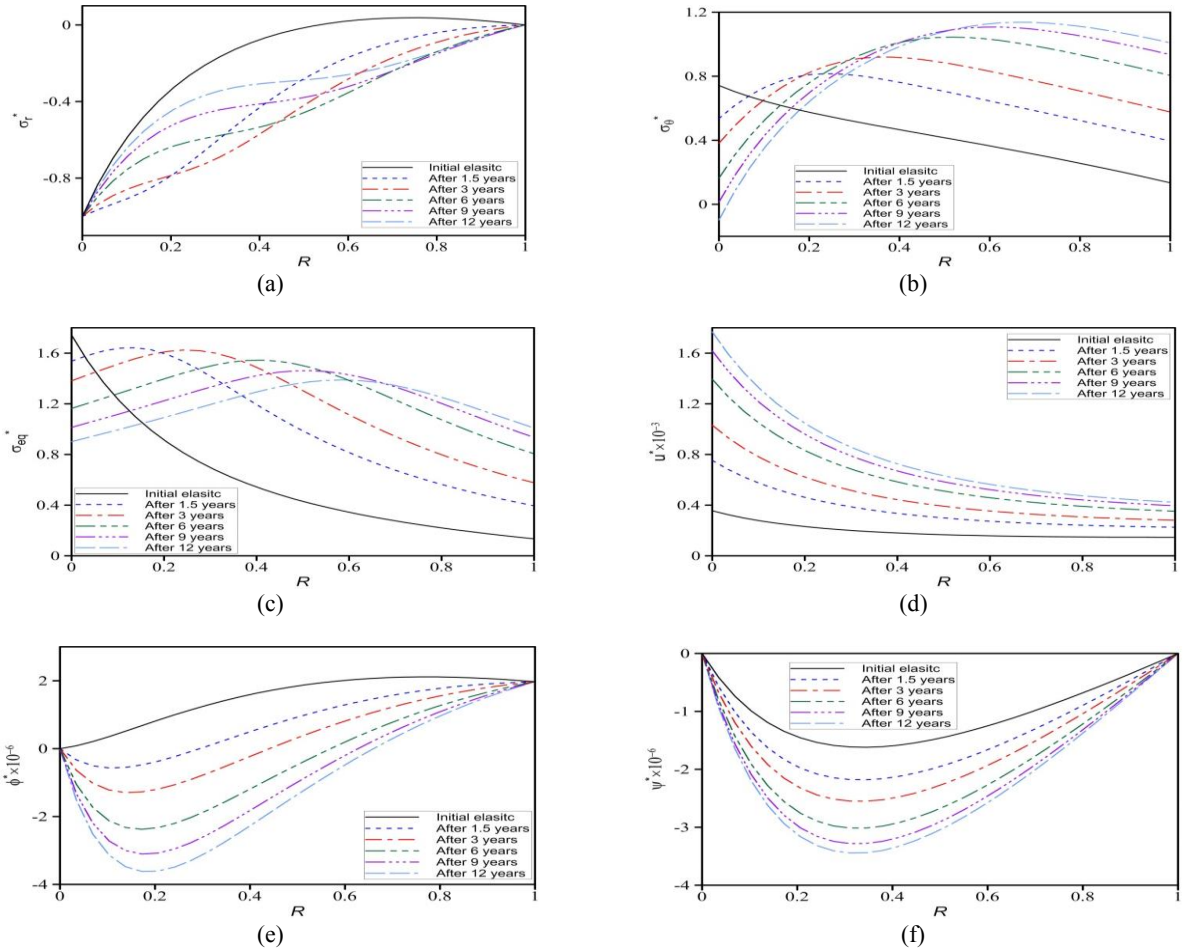

Fig.1
(a) Radial, (b) circumferential and (c) equivalent creep stresses, (d) radial displacement (e) electric and (f) magnetic potentials redistribution during creep progress.

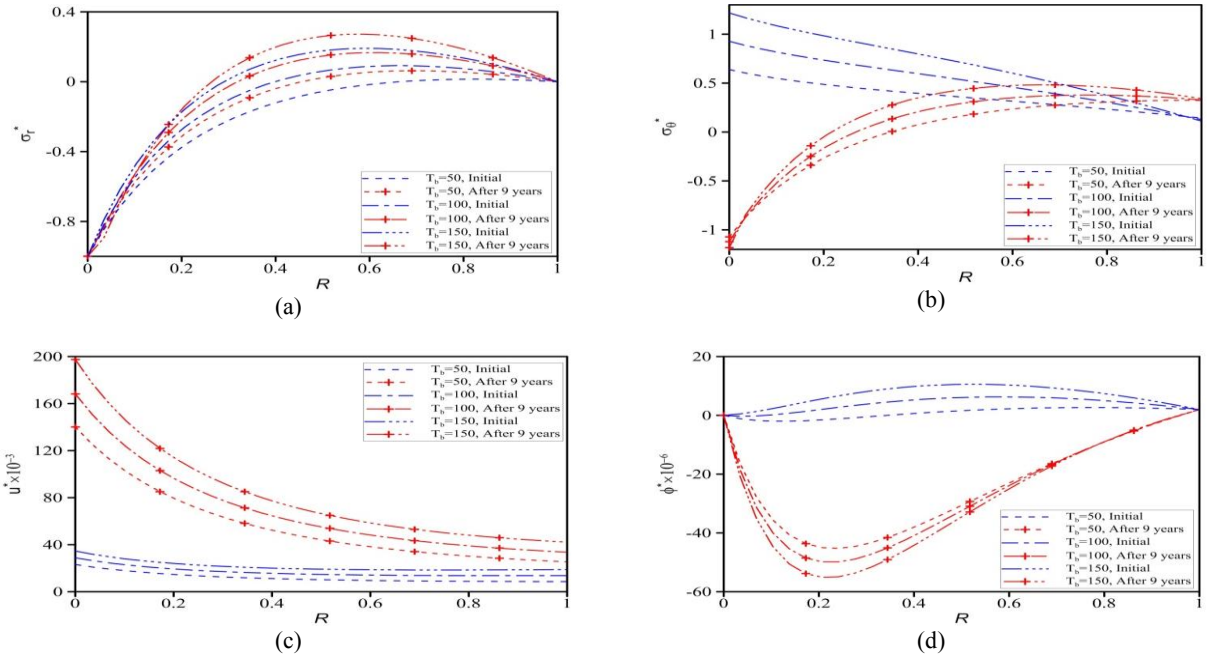

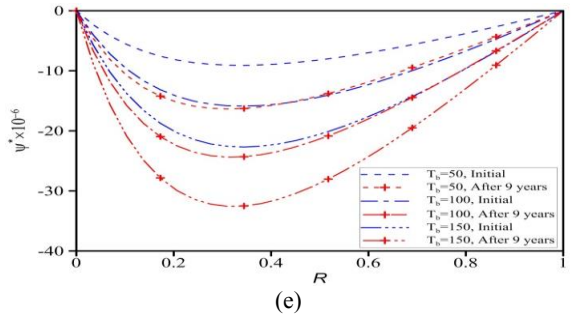

(e)

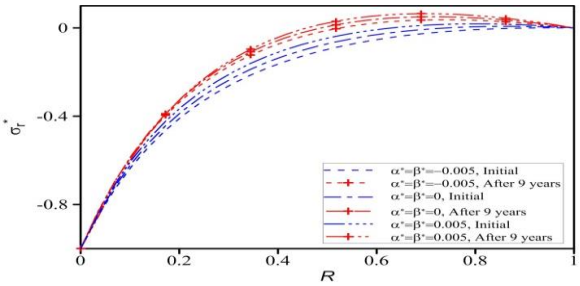

(a)

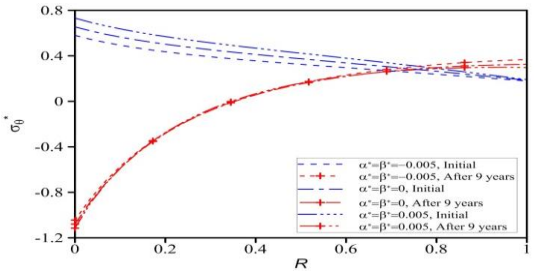

(b)

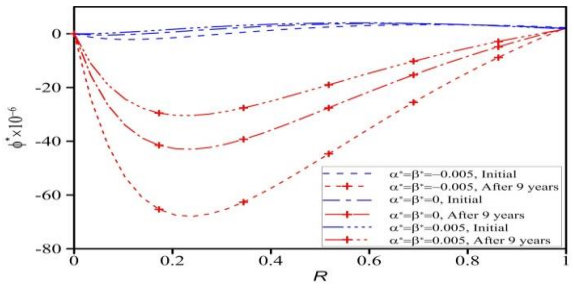

(c)

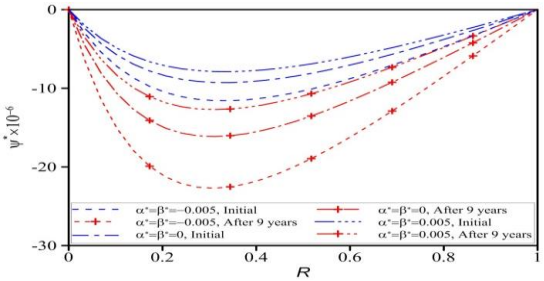

(d)

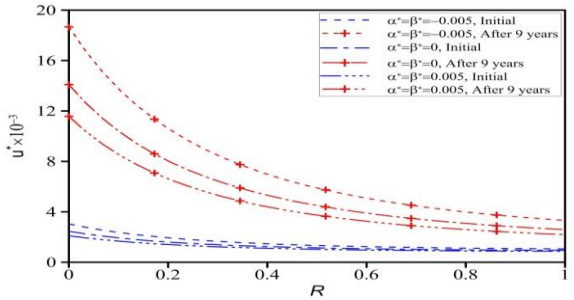

(e)

Fig.2
Influence of hygrothermal condition on initial and creep (a) Radial stress, (b) circumferential stress (c) radial displacement (d) electric potential and (e) magnetic potential.

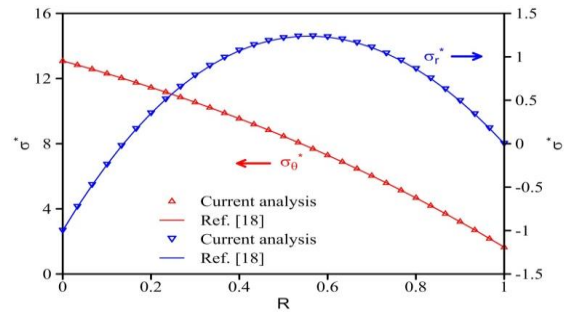

Fig.3
Influence of hygrothermal dependence of the elastic coefficients on the initial and creep (a) Radial stress, (b) circumferential stress (c) electric potential, (d) magnetic potential and (e) radial displacement distributions.

Fig.4
Radial and circumferential stresses.

4 CONCLUSION

In this article, the time-dependent creep progress of a magneto-electro-elastic hollow sphere is investigated analytically. The sphere is considered to be subjected to magneto-electro-mechanical loading and is placed in a hygrothermal environmental condition. The creep analysis is carried out using the Prandtl-Reuss equations as well as Norton's law. It is observed that variations in the rate of stresses, electric and magnetic potentials and displacement, regardless of the value, become less extensive during the time. Also, the increase in tensile hoop stress, resulted from creep progress, must be considered in design progress because of the role of the circumferential stress in the failure of spheres. Results show that the effect of hygrothermal loading after creep progress must be considered in design to avoid failure because of tensile radial stress. The effect of hygrothermal loading is more extensive after creep evolution. As observed, the negative value of empirical constant increases the radial stress, radial displacement, electric potential and magnetic potential and decreases the hoop stress. While, the positive one has a reverse effect.

REFERENCES

[1] Saadatfar M., Aghaie-Khafri M., 2015, Electro magneto thermo elastic behavior of a rotating imperfect hybrid functionally graded hollow cylinder resting on an elastic foundation, *Smart Structures and Systems* **15**:1411-1437.

[2] Saadatfar M., Aghaie-Khafri M., 2015, On the magneto-thermo-elastic behavior of a FGM cylindrical shell with pyroelectric layers featuring interlaminar bonding imperfections rested in an elastic foundation, *Journal of Solid Mechanics* **7**: 344-363.

[3] Saadatfar M., 2018, Effect of interlaminar weak bonding and constant magnetic field on the hygrothermal stresses of a FG hybrid cylindrical shell using DQM, *Journal of Stress Analysis* **3**: 93-110.

[4] Ghorbanpour Arani A., Mosallaie Barzoki A.A., Kolahchi R., Mozdianfard M.R., Loghman A., 2011, Semi-analytical solution of time-dependent electro-thermo-mechanical creep for radially polarized piezoelectric cylinder, *Computers & Structures* **89**: 1494-1502.

[5] Smittakorn W., Heyliger P.R., 2000, A discrete-layer model of laminated hygrothermo piezoelectric plates mech, *Composite Materials and Structures* **7**: 79-104.

[6] Smittakorn W., Heyliger P.R., 2001, An adaptive wood composite: theory, *Wood Fiber Science* **33**: 595-608.

[7] Raja S., Sinha P.K., Prathap G., Dwarakanthan D., 2004, Thermally induced vibration control of composite plates and shells with piezoelectric active damping, *Smart Materials and Structures* **13**: 939-950.

[8] Dai H.L., Wang X., 2006, Magneto–thermo–electro–elastic transient response in a piezoelectric hollow cylinder subjected to complex loadings, *International Journal of Solids and Structures* **43**: 5628-5646.

[9] Akbarzadeh A.H., Chen Z.T., 2012, Magneto electro elastic behavior of rotating cylinders resting on an elastic foundation under hygrothermal loading, *Smart Materials and Structures* **21**: 125013.

[10] Akbarzadeh A., Chen Z., 2014, Thermo-magneto-electro-elastic responses of rotating hollow cylinders, *Mechanics of Advanced Materials and Structures* **21**: 67-80.

[11] Saadatfar M., Aghaie-Khafri M., 2015, On the behavior of a rotating functionally graded hybrid cylindrical shell with imperfect bonding subjected to hygrothermal condition, *Journal of Thermal Stresses* **38**: 854-881.

[12] Saadatfar M., Aghaie-Khafri M., 2015, Hygrothermal analysis of a rotating smart exponentially graded cylindrical shell with imperfect bonding supported by an elastic foundation, *Aerospace Science and Technology* **43**: 37-50.

[13] Saadatfar M., 2015, Effect of multiphysics conditions on the behavior of an exponentially graded smart cylindrical shell with imperfect bonding, *Meccanica* **50**: 2135-2152.

[14] Wang H.M., Ding H.J., 2006, Transient responses of a magneto-electro-elastic hollow sphere for fully coupled spherically symmetric problem, *European Journal of Mechanics A/Solids* **25**: 965-980.

[15] Wang H.M., Ding H.J., 2007, Radial vibration of piezoelectric/magneto strictive composite hollow sphere, *Journal of Sound Vibration* **307**: 330-348.

[16] Ootao Y., Ishihara M., 2012, Exact solution of transient thermal stress problem of a multilayered magneto-electro-thermoelastic hollow sphere, *Applied Mathematical Modeling* **36**: 1431-1443.

[17] Chen J.Y., Pan E., Heyliger P.R., 2015, Static deformation of a spherically anisotropic and multilayered magneto-electro-elastic hollow sphere, *International Journal of Solids and Structures* **60**: 66-74.

[18] Saadatfar M., Aghaie-Khafri M., 2014, Hygrothermo magneto electro elastic analysis of a functionally graded magneto electro elastic hollow sphere resting on an elastic foundation, *Smart Materials and Structures* **23**: 035004.

[19] Saadatfar M., 2019, Stress redistribution analysis of piezomagnetic rotating thick-walled cylinder with temperature-and moisture-dependent material properties, *Journal of Applied and Computational Mechanics* **6**: 90-104.

[20] Ghorbanpour Arani A., Kolahchi R., Mosallaie Barzoki A.A., Loghman A., 2013, The effect of time-dependent creep on electro-thermo-mechanical behaviors of piezoelectric sphere using Mendelson's method, *European Journal of Mechanics A/Solids* **37**: 318-328.

[21] Jabbari M., Tayebi M.S., 2016, Time-dependent electro–magneto–thermo elastic stresses of a poro-piezo-functionally graded material hollow sphere, *Journal of Pressure Vessel Technology* **138**: 051201.

[22] Loghman A., Tourang H., 2016, Non-stationary electro-thermo-mechanical creep response and smart deformation control of thick-walled sphere made of polyvinylidene fluoride, *Journal of Brazilian Society of Mechanical Science and Engineering* **38**:2547-2561.

[23] Saadatfar M., Rastgoo A., 2008, Stress in piezoelectric hollow sphere with thermal gradient, *Journal of Mechanical Science and Technology* **22**: 1-8.

[24] Bakhshizadeh A., Zamani Nejad M., Davoudi Kashkoli M., 2017, Time-dependent hygro-thermal creep analysis of pressurized fgm rotating thick cylindrical shells subjected to uniform magnetic field, *Journal of Solid Mechanics* **9**: 663-679.

[25] Shariyat M., Ghafourinam M, 2019, Hygrothermo mechanical creep and stress redistribution analysis of thick-walled FGM spheres with temperature and moisture dependent material properties and inelastic radius changes, *International Journal of Pressure Vessels and Piping* **169**: 94-114.

[26] Saadatfar M., 2019, Time-dependent creep response of magneto-electro-elastic rotating disc in thermal and humid environmental condition, *AUT Journal of Mechanical Engineering*.(In Press)

[27] Ghorbanpour A., Golabi S., Saadatfar M., 2006, Stress and electric potential fields in piezoelectric smart spheres, *Journal of Mechanical Science and Technology* **20**: 1920-1933.